Hindawi
Journal of Chemistry
Volume 2020, Article ID 1942791, 13 pages
https://doi.org/10.1155/2020/1942791

Research Article

Application of Nanoscale Zwitterionic Polyelectrolytes Brush with High Stability and Quantum Yield in Aqueous Solution for Cell Imaging

Zhiyong Zhang,[1] Minqiang Tan,[2] Linghui Kong,[2] Xiaomei Lu,[3] Pengfei Sun,[4] Hua Mo,[2] Quli Fan ,[4] and Wei Huang[5]

[1]*Inner Mongolia Power Research Institute, Hohhot 010020, China*
[2]*Appraisal Central for Environment & Engineering, Ministry of Ecology and Environment, Beijing 100112, China*
[3]*Key Laboratory of Flexible Electronics (KLOFE) & Institute of Advanced Materials (IAM), Jiangsu National Synergetic Innovation Center for Advanced Materials (SICAM), Nanjing Tech University (NanjingTech), 30 South Puzhu Road, Nanjing 211816, China*
[4]*Key Laboratory for Organic Electronics and Information Displays & Jiangsu Key Laboratory for Biosensors, Institute of Advanced Materials (IAM), Jiangsu National Synergetic Innovation Center for Advanced Materials (SICAM), Nanjing University of Posts & Telecommunications, 9 Wenyuan Road, Nanjing 210023, China*
[5]*Shaanxi Institute of Flexible Electronics (SIFE), Northwestern Polytechnical University (NPU), 127 West Youyi Road, Xi'an 710072, Shanxi, China*

Correspondence should be addressed to Quli Fan; iamqlfan@njupt.edu.cn

Received 12 July 2019; Accepted 18 December 2019; Published 27 February 2020

Academic Editor: Georgios Matthaiolampakis

Cationic and zwitterionic polyelectrolytes are synthesized through atom transfer radical polymerization (ATRP), comprising a polyfluorene backbone with a small fraction of 2,1,3-benzothiadiazole and poly[2-(dimethylamino)ethyl methacrylate] (PDMAEMA) side chains. Due to higher charge density generated from grafted side chains, two polymers show higher water solubility and higher quantum yield. In comparison with cationic polyelectrolytes, zwitterionic polyelectrolytes are stable over a broad pH range from 1 to 13, even in 1 M NaCl solution. The absence of FRET between zwitterionic polymers and dye-labeled ssDNA indicates their ultralow nonspecific adsorption, while cationic polymer shows much stronger nonspecific interactions. The MTT assay of zwitterionic polymers exhibits their minimal cytotoxicity and potential in long-term clinical application. Most importantly, zwitterionic polymer could be efficiently taken up by cells, whereas cationic polymer stains the surface of cell due to membrane disruption generated from positive charges. The results illustrate that conjugated zwitterionic polymer could serve as a novel type of highly efficient ultralow fouling material with low cytotoxicity for labelling cell or potential biomedical applications.

1. Introduction

Cationic materials have been extensively used as transport materials crossing the cell membranes for labelling cell or gene delivery due to electrostatic attraction between positive charge of cationic materials and negative charge of cell membrane [1–3]. However, electrostatic attraction as a nonspecific force induces undesired interactions and then influences efficiency of detection or drug delivery. Meanwhile, the cytotoxicity generated from positive charge limits their biomedical applications significantly. Therefore, obtaining a kind of antifouling materials with low cytotoxicity for further applications such as cell imaging and drug delivery is still desired.

Recently, zwitterionic materials have attracted considerable interest due to their remarkable application potential in polymer light-emitting diodes (PLED), biosensors, and drug delivery [4, 5]. Compared with anionic or cationic

materials, zwitterions generally exhibit the following unique properties: (1) highly biocompatible and remarkably resistant to nonspecific protein adsorption and bacterial/cell adhesion due to strong hydration layer or superhydrophilic nature [6, 7]; (2) being inert with respect to most bioconjugation reaction systems due to the absence of any primary amine and carboxylic acids [8]; (3) allowing for the stability over the broad pH range for sulfobetaine components [8]; and (4) stability at high salt concentrations [8, 9]. These unique characters endow zwitterion-based materials with enormous potential in biological applications.

Conjugated polyelectrolytes (CPEs) as an essential candidate for fluorescent materials often refer to a kind of macromolecules with a conjugated polymeric backbone and side chains including anionic or cationic groups [10–14]. Pendant hydrophilic segments of CPEs offer them solubility in high polarity solvents, but their lower water-solubility, bad mechanical stability, phase separation, and amorphous in aqueous media induced by the hydrophobicity of a high rigid main chain significantly hinder their biological applications. In view of this, CPEs with more ionic pendant side chains and zwitterions would be an intriguing choice. Combining zwitterions with the nature of resistant to nonspecific adsorption and fluorescence conjugated polymer, it will develop conjugated polyelectrolytes as low cytotoxicity and nonfouling materials for various biological applications.

In this paper, we report two new polyelectrolytes including a small fraction of 4,7-dibromo-2,1,3-benzothiadiazole (BT), cationic and zwitterionic polyfluorene-grafted-poly(2-(dimethylamino)ethyl methacrylate) (PF-*g*-PDMAEMA). The integration of BT units into conjugated backbones is to more clearly investigate stability of zwitterionic polyelectrolytes in aqueous solution. Since aggregation generated from complexation between CPEs and target molecules favors intrachain or interchain FRET from the fluorene segments to the BT units, inducing the fluorescence changes from blue to green [15, 16]. To certify nonfouling nature of zwitterionic polymers, cationic polymers with the same backbones structure are also synthesized. We find that due to the high charge density stemmed from PDMAEMA graft side chains by atom transfer radical polymerization, both cationic and zwitterionic polymers exhibit excellent water-solubility and much higher quantum yield in aqueous solution. And optical experiments prove the stability of zwitterionic polymer in aqueous solution with different pH and concentrations of NaCl. Furthermore, FRET, cell viability, and cell imaging experiments demonstrate that zwitterionic polymer shows minimal nonspecific interactions with DNA, low cytotoxicity, and cellular uptake, respectively. These desirable properties of zwitterionic polymer ensure their potential applications in sensing and drug delivery. Most importantly, this study highlights a novel concept for designing CPEs with desirable material in biomedical applications.

2. Results and Discussion

2.1. Synthesis and Characterization. The chemical structures of P4 and P4′ are shown in Scheme 1. Scheme 2 depicts the synthetic routes toward P4 and P4′. The monomers, 2,7-dibromo-9,9-bis(3-hydroxylpropyl)-fluorene (M2) and 9,9-dioctylfluorene-2,7-bis(trimethylene boronate) (M3), were synthesized according to our previous report. The Suzuki cross-coupling copolymerization of M2, M3, and 4,7-dibromo-2,1,3-benzothiadiazole at a feed ratio of 1 : 0.98 : 0.2 gave the neutral statistical random copolymer, P1. Further treatment of P1 with 2-bromoisobutyryl bromide in the presence of triethylamine in THF provided P2. The chemical structures of P1 and P2 were characterized by ^{1}H NMR and ^{13}C NMR. The number-average molecular weight and polydispersity of P2 are 31000 g/mol and 1.9, respectively, measured by GPC using THF as the eluent and polystyrene as the standard. ATRP of P2 with DMAEMA was performed in o-dichlorobenzene at 90°C for 12 h using 1,1,4,7,10,10-hexamethyl triethylenetetramine (HMTETA) as the ligand and CuBr as the catalyst. The resulting solution was purified through a column of neutral alumina and precipitated in n-hexane, yielding P3 as light yellow fibers. P3 was further treated with 1,3-propanesultone in acetonitrile at room temperature for 12 h. Water was added into the solution and precipitation was disappeared and kept stirring for 24 h. After purification by dialysis against deionized water using an 8.0 kDa molecular weight cutoff dialysis membrane for 3 days and then freeze-drying, finally P4 was obtained as yellow powder. P4′ was synthesized by reacting P3 with methyl iodide at room temperature for 4 h.

The chemical structures of P3, P4, and P4′ were determined by ^{1}H NMR. As compared to P3, three new peaks at 3.83, 2.99, and 2.30 ppm appearing in the ^{1}H NMR of P4 are assigned to $-N(CH_3)_2CH_2CH_2CH_2SO_3$, $-N(CH_3)_2CH_2CH_2CH_2SO_3$, $-N(CH_3)_2CH_2CH_2CH_2SO_3$, respectively, while peaks assigned to $-OCH_2-$ and $-CH_2N(CH_3)_2CH_2$ shift 4.60 and 3.83 ppm, respectively. The integral ratio of the peak at 2.30 ppm to that at 3.25 ppm (corresponding to the methyl protons close to nitrogen atom) is close to 1 : 3, showing that the degree of quantification is ~100%. For P4′, the ratio of integrated areas of methyl ($-NCH_3$) (3.32 ppm) and methylene ($-CH_2N$) (3.90 ppm) peaks in ^{1}H NMR exhibits that the degree of quaternization is higher than 95%. However, in ^{1}H NMR of both P4 and P4′, the signals of protons assigned to conjugated backbones are more difficult to discern. This result may be ascribed to two factors. One is few protons on the fluorene rings relative to the much greater number of protons on the side chains. The other is restricted mobility, resulting in peak broadening and thus substantially weaker signals of the protons of fluorene unit [17]. Detailed ^{1}H NMR spectra are shown in Figure 1.

The number-average molecular weights P4 was determined by high performance liquid chromatography (HPLC) in water (1 M $NaNO_3$) using poly(ethylene glycol) standards to obtain a molecular weight (Mn = 321 800, Mw/Mn = 1.0). The number-average molecular weights P4′ was also determined by high performance liquid chromatography (HPLC) in water (1 M $NaNO_3$) using poly(ethylene glycol) standards to obtain a molecular weight (Mn = 319 900, Mw/Mn = 1.1), corresponding to a degree of polymerization of ~1200. This result reveals that there are an average monomer number of 40 per two fluorene units.

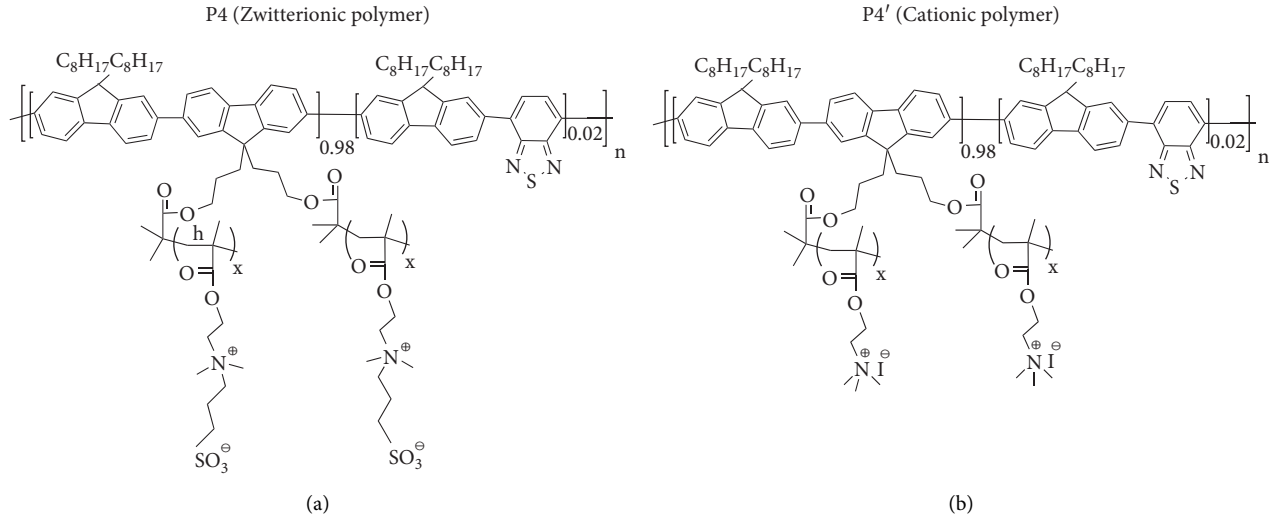

Scheme 1: The chemical structures of P4 and P4′.

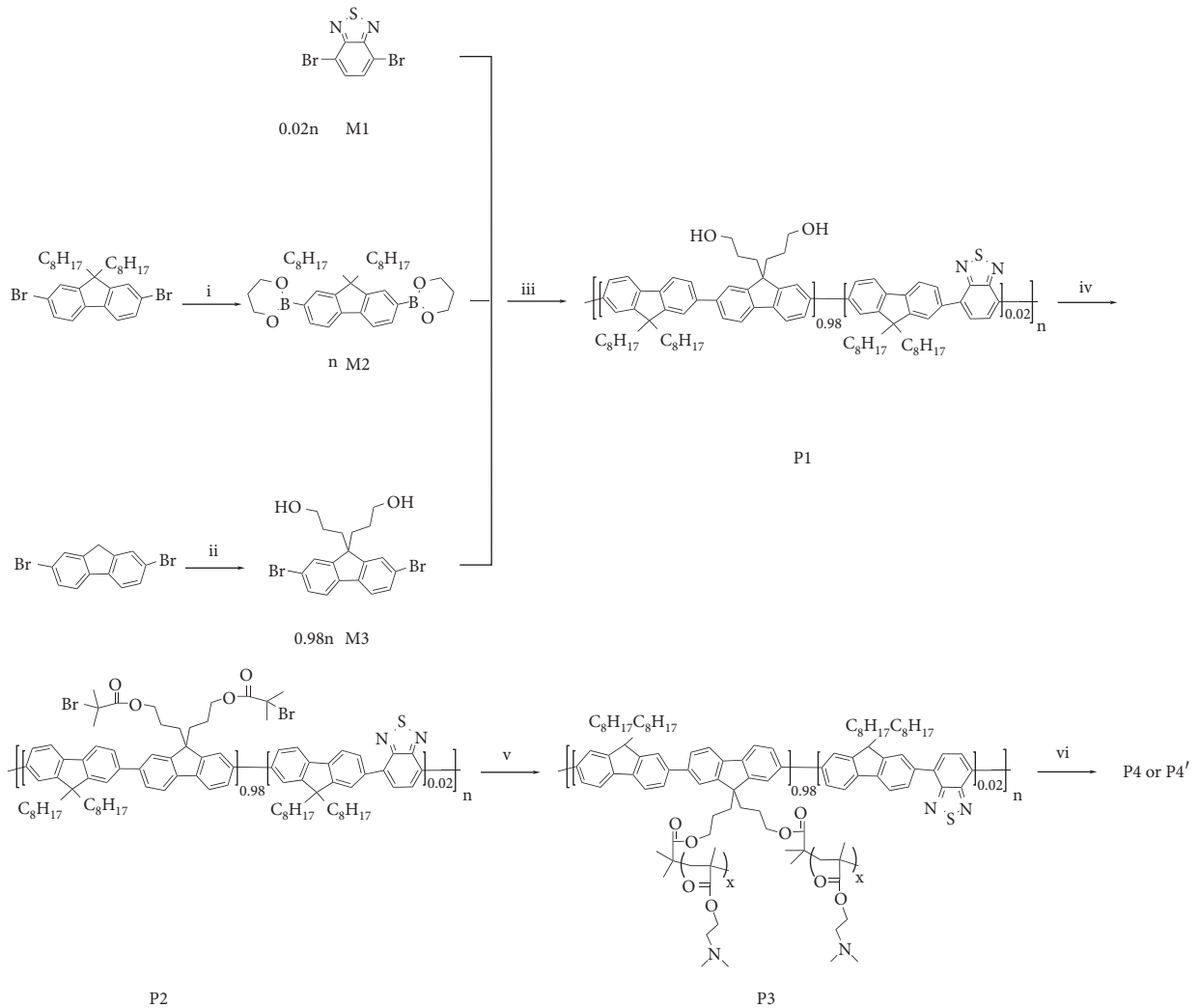

Scheme 2: The synthetic routes toward P4. Reagents and conditions: (i) (1) n-BuLi, THF, -78 °C, 2 h; (2) triisopropyl borate, room temperature, 12 h; (3) 1,3-propanediol, toluene, reflux, 10 h; (ii) 3-bromo-1-propanol, tetrabutylammonium bromide, NaOH/H_2O, DMSO, 85°C, 24 h; (iii) $Pd(PPh_3)_4$, K_2CO_3, toluene/H_2O, 90°C, 72 h; (iv) 2-bromoisobutyryl bromide, $N(Et)_3$, 24 h; (v) CuBr, HMTETA, DMAEMA, 90°C, 12 h; (vi) 1,3-propanesultone, acetonitrile, room temperature, 36 h.

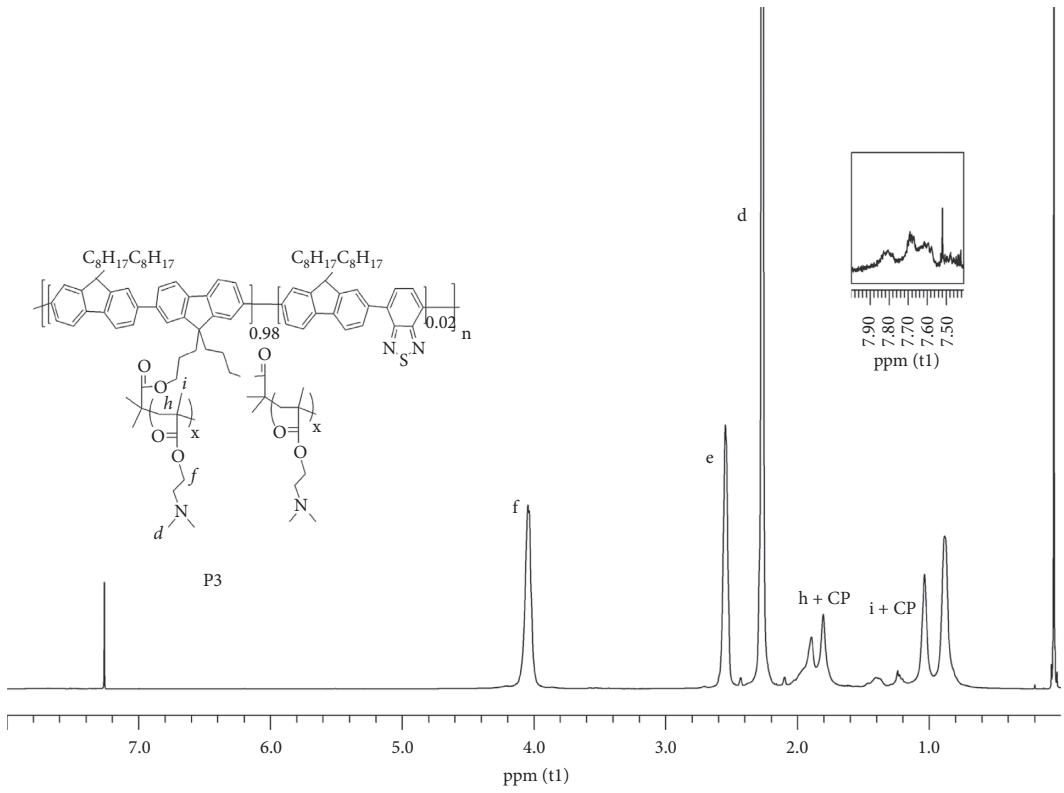

(a)

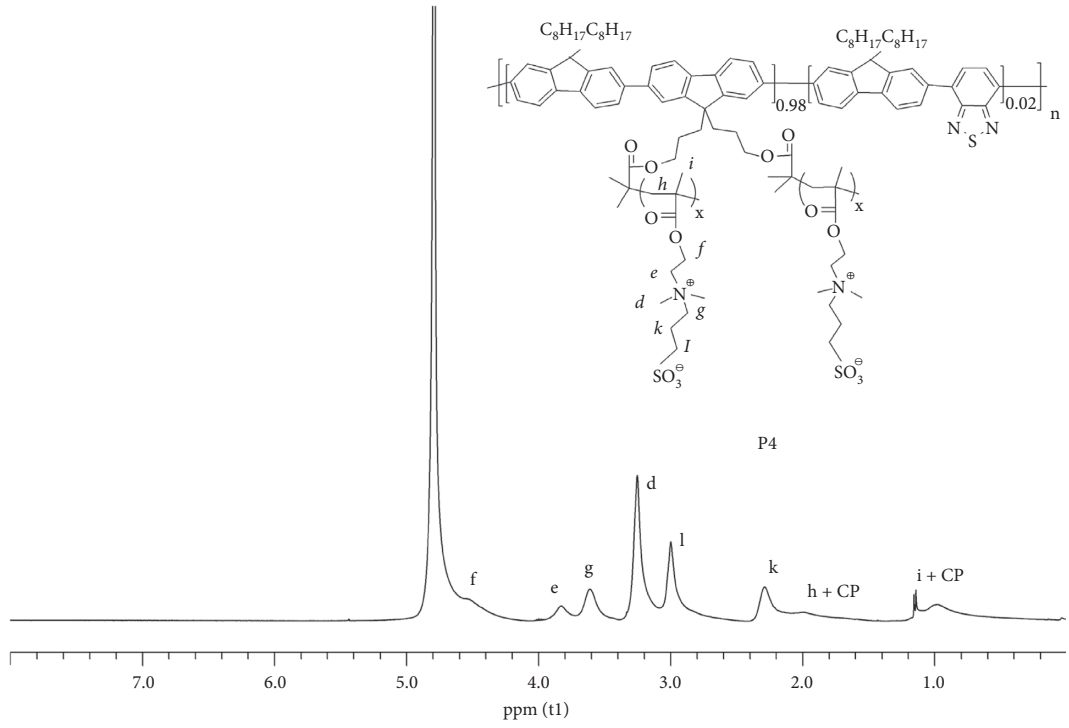

(b)

Figure 1: Continued.

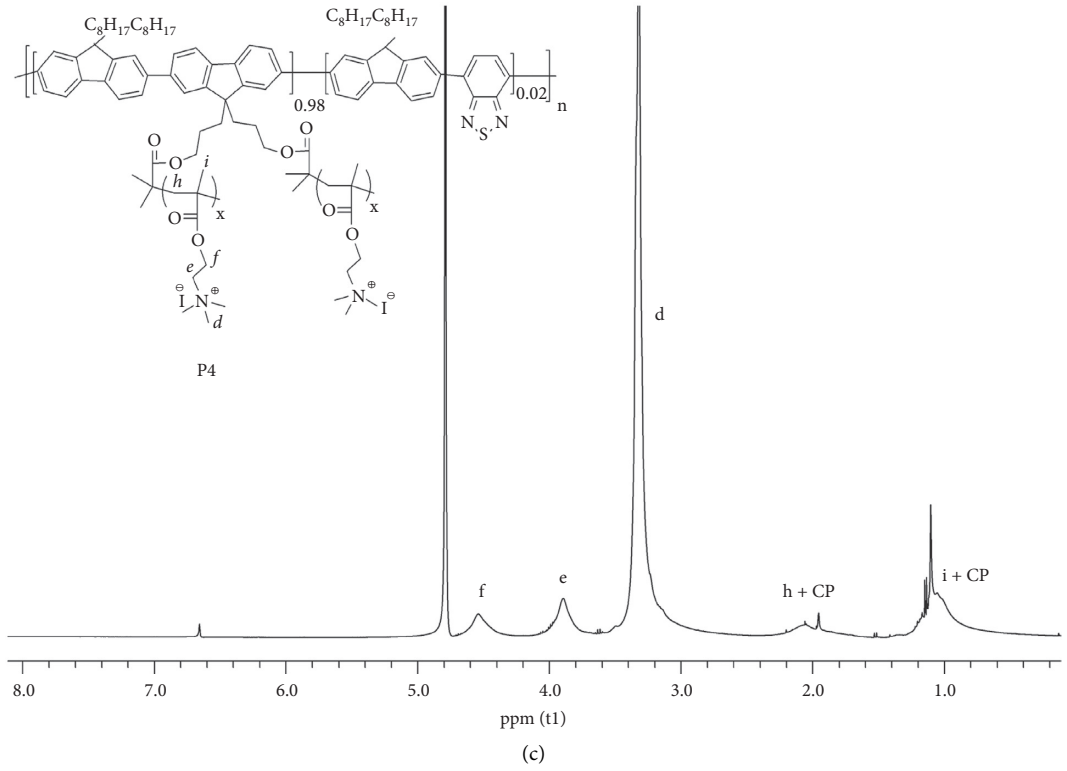

Figure 1: ^{1}H NMR of P3 (in $CDCl_3$), P4 (in H_2O), and P4′ (in H_2O); CP refers to alkyl chains on the fluorene units.

2.2. Self-Assembly Properties. The self-assembly behaviors of P4 and P4′ in aqueous solution are investigated by dynamic light scattering (DLS). Figure 2 gives the hydrodynamic radius distribution of P4 and P4′ in water at the concentration of 2 μM based on repeat unit (RU). Unimodal distribution reveals the formation of micellar nanoparticles with the diameter of about 30 nm, respectively. The similar hydrodynamic diameters of both polymers in aqueous solution demonstrate that the difference in ionic groups does not affect their status in solution. Tapping-mode atomic force microscopy (AFM) observations have been performed to examine the morphologies of P4 and P4′ in dry state after depositing onto mica. Figure 3 display the spherical morphology of P4 and P4′ with a uniform diameter of 50 nm, while the AFM height image reveals the vertical height of 5 to 10 nm. The difference between diameter and height may originate from the nanoparticles collapse upon transforming from solution state into dry state. These observations just account for the larger diameter by AFM relative to that from the DLS data. Meanwhile, transmission electron microscopy studies (Figure 4) also indicate spherical morphologies with diameters of about 40 nm for P4 and P4′. These data vividly demonstrate that P4 and P4′ possess excellent dispersity in aqueous solution.

2.3. Optical Properties. The UV-vis absorption and photoluminescence (PL) spectra of P4 and P4′ in water are shown in Figure 5. The polymer concentration based on repeating unit (RU) is 10 μM. The absorption spectra of P4 and P4′ exhibit the same maxima at 384 nm corresponding to the fluorene segments, but characteristic band ranging from 426 to 520 nm ascribed from BT units can only obviously be observed in the absorption spectra of P4′. The emission spectra of P4 and P4′ also show the same maxima at 425 nm, but obvious emission band in 500–650 nm region can be observed in the emission spectrum of P4. Differences on optical properties of two polymers may depend on their status in solution because of the stronger ion-ion association existing in the solution of zwitterionic polymer [18].

The presence of the peaks at 425 nm and 540 nm suggests efficient FRET from fluorene moiety to BT units for P4. Time-resolved PL spectroscopy are obtained by exciting at 380 nm and monitoring at 420 nm to provide direct information of FRET [19, 20]. As shown in Figure 6, the fluorescence decay kinetics of P4 exhibit a two-exponential decay model with lifetimes of 0.29 (27%) and 0.63 ns (73%), whereas those of P4′ are observed as a one-exponential time decay with a lifetime of 0.54 ns. The short lifetime indicates that efficient FRET occurs in P4 aqueous solution, which is probably attributed to intrachain interactions of polymer due to no aggregation in P4 aqueous solution demonstrated by DLS analysis. Thus, it should be suggested that zwitterionic groups could obviously affect intrachain behavior of polymer.

2.4. Zeta Potential. For most conjugated polyelectrolytes, salt could influence their solution behavior in aqueous solution as it results in a screening of repulsion and polyelectrolytes will precipitate from solution. Since zwitterionic polymers carry equal numbers of positive and negative

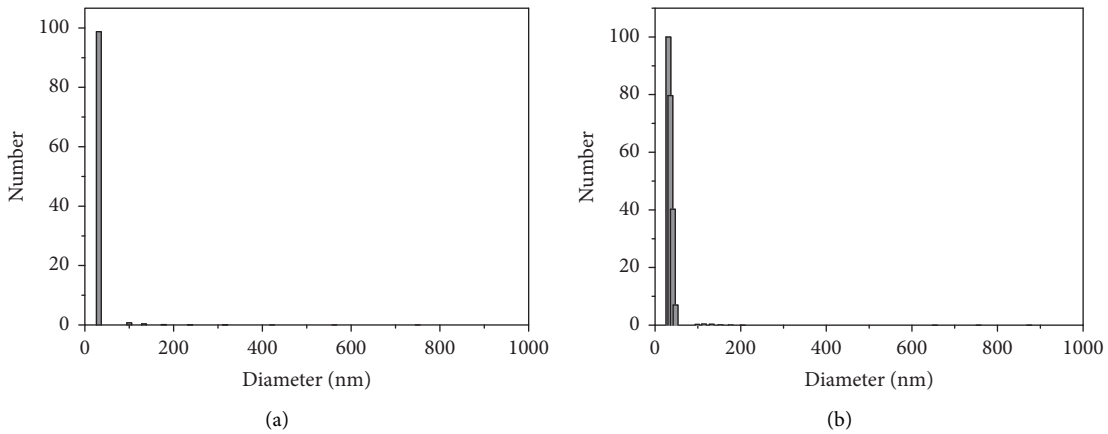

Figure 2: Hydrodynamic radius distribution of P4 (a) and P4′ (b) in water at [RU] = 1 μM.

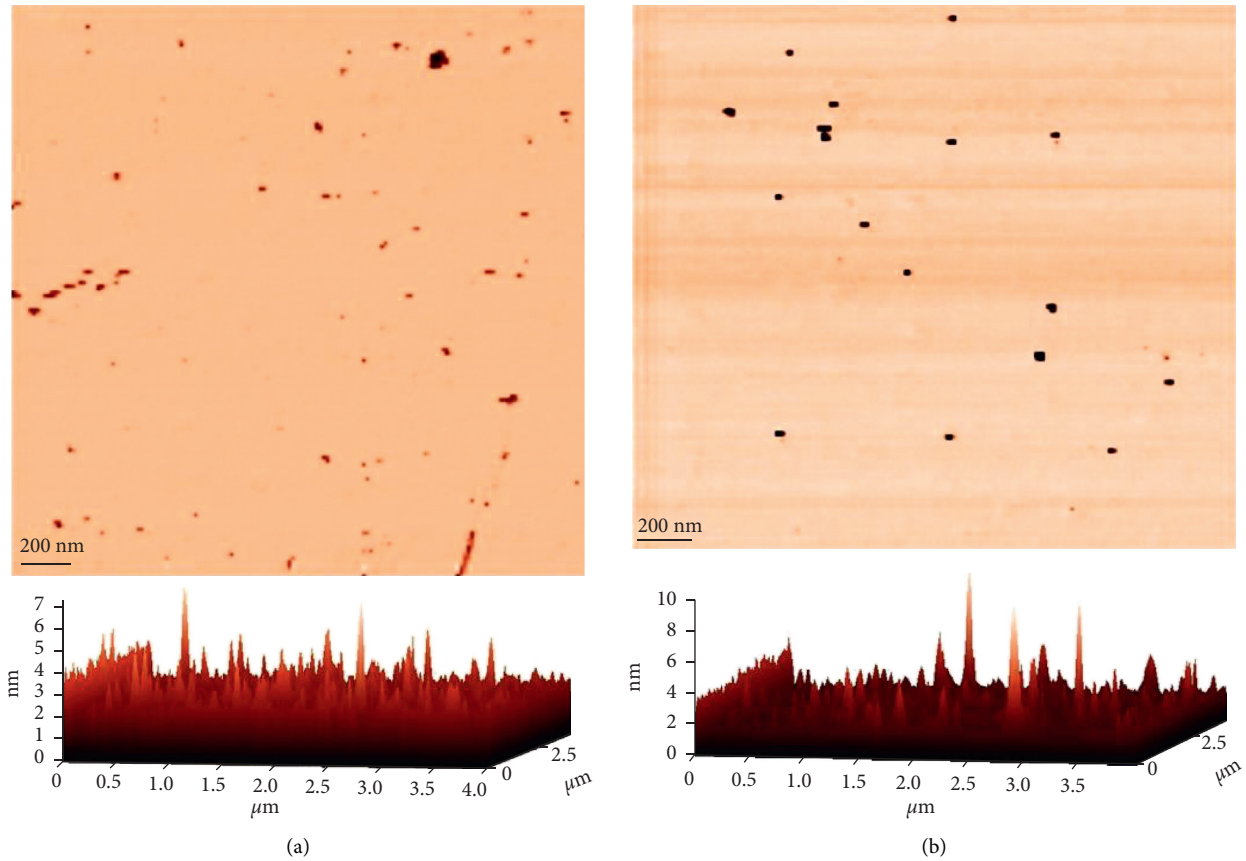

Figure 3: AFM image of P4 (a), phase image (top), and height image (bottom); AFM image of P4′ (b) phase image (top) and height image (bottom).

charges on the same monomer, the attraction between ammonium and sulfonate of the same or distinct monomer or polymer side chains is generally considered as giving them a net charge of zero and thus induce insolubility of polyzwitterion and zero zeta potential [21]. However, zeta potential analysis shows a P4 has high positive zeta potential of +38.4 mv in deionized water, which may be ascribed to incomplete quaternization of tertiary amine. However, ^{1}H NMR indicates no reliable proof of incomplete quaternization and thus positive zeta potential may be not generated from the protonation of tertiary amine. This phenomenon is also observed by the previous literature [18].

2.5. Water-Solubility and Quantum Yield. For CPEs, serving as efficient materials in sensing applications, better water-solubility and higher quantum yield are vital. However, polymer aggregation in aqueous solution due to the

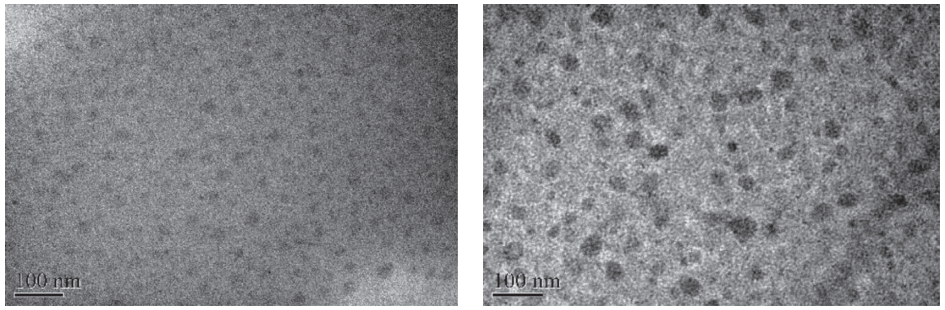

(a) (b)

Figure 4: Typical TEM images of P4 (a) and P4′ (b).

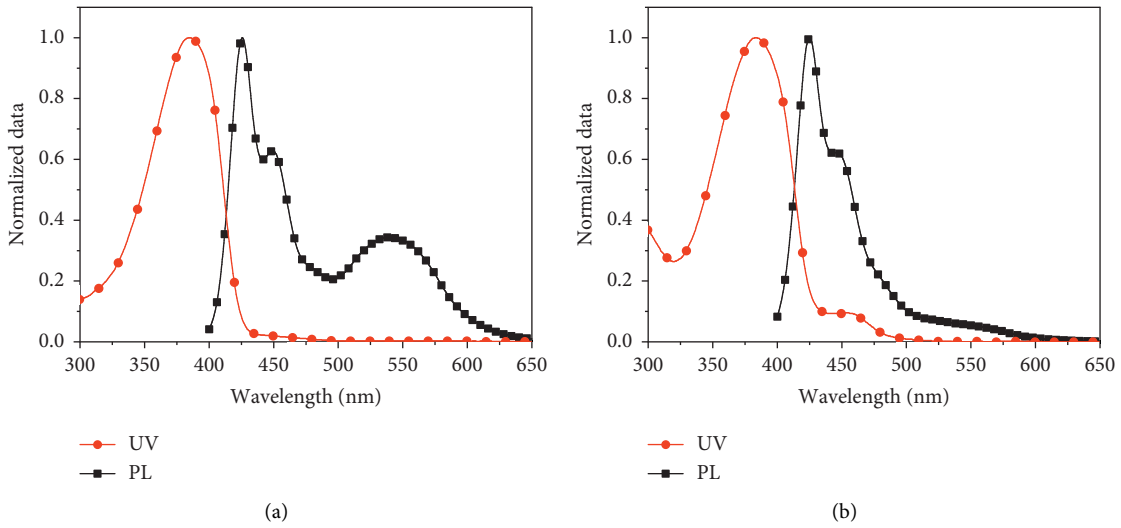

(a) (b)

Figure 5: The UV-vis absorption and PL spectra P4 (a) and P4′ (b) in water (excitation at 384 nm).

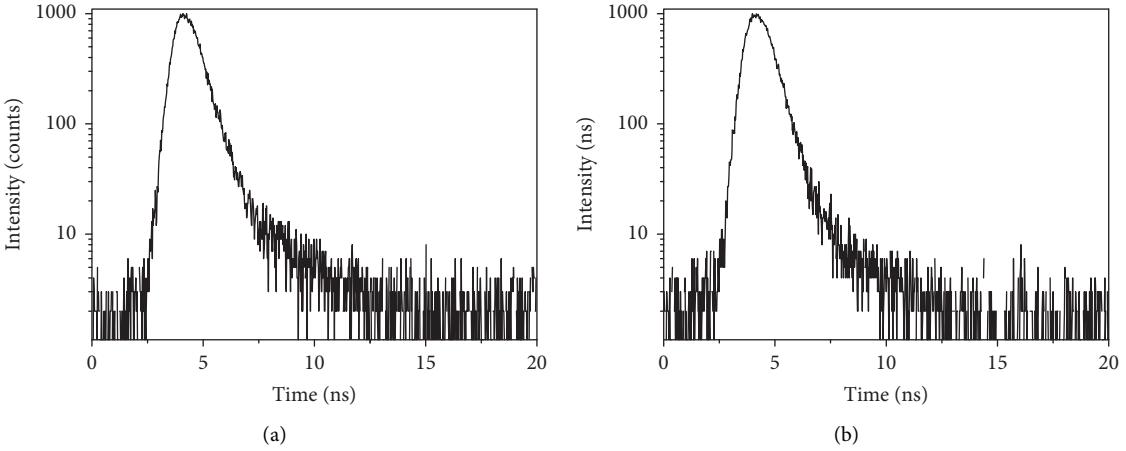

(a) (b)

Figure 6: Fluorescence decay curves of P4 (a) and P4′ (b) in dilute solution.

hydrophobic nature of aromatic conjugated backbones dramatically limits the solubility of CPEs in water, consequently weak quantum yield [22]. Therefore, improving water-solubility of polymer can decrease the polymer aggregation in aqueous solution, which will favor to the realization of higher quantum yield.

The solubility limits of P4 and P4′ in water at 25°C are ~36 and 32 mg/mL, respectively. As confirmed by dynamic

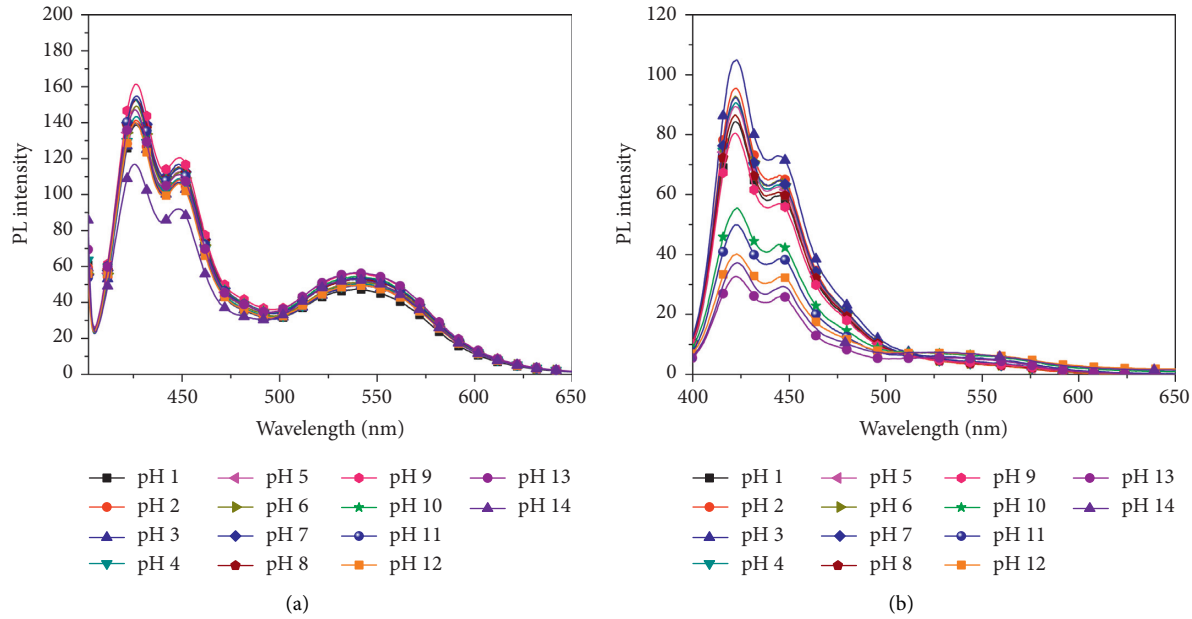

Figure 7: Emission spectra of P4 (a) and P4′ (b) (excitation at 384 nm) at different pH values.

light scattering (DLS), the diameters for P4 and P4′ in water indicate that two polymers have a well-extended chain conformation in aqueous solution, which originates from bulky hydrophilic segments and meanwhile electrostatic repulsion also favors a stretching of chains. The PL quantum yields for P4 and P4′ in water were determined to be 45 and 42%, respectively, using quinine sulfate in 0.1 M H_2SO_4. Weakened polymer aggregation due to better water-solubility gives the higher PL quantum yields of P4 and P4′. In addition, many grafted side chains construct an effective hydrophilic layer that wraps the hydrophobic backbone, providing efficiently protective layers for the conjugated backbones against the diffusion of water molecules. As such, the reduced charge-transfer character of excited states also is devoted to higher PL quantum yields [22].

2.6. pH-Influenced Photoluminescence. The effect of pH on the fluorescence intensity of P4 and P4′ was investigated in a range of pH from 1 to 14. As shown in Figure 7(a), there is nearly not any change in the fluorescence intensity of P4 over the pH range 1–13 and slightly decreased fluorescence intensity when the pH is up to 14, which demonstrate that zwitterionic components can effectively inhibit aggregation and thus provide stability of conjugated electrolyte brush over a broad pH range. In contrast, P4′ starts to become unstable at pH 10, showing significantly decreased fluorescence intensity at 425 nm and increased fluorescence intensity at 540 nm (Figure 7(b)). The reduced fluorescence intensity should be resulted from neutralization of quaternized ammonium group by OH^- in an alkaline environment and thus the formation of interchain aggregation [23]. To clearly describe the difference in emission spectra between P4 and P4′ over the pH range 1–14, the value of I_{540nm}/I_{425nm} (I refers to fluorescence intensity) as a function of pH is depicted in Figure 8. In comparison with P4′, P4 is still stable in a range of pH from 1 to 13 and insensitive to pH. As measured by DLS (Table 1), the diameter of P4 in a range of pH from 1 to 13 remains significantly unchanged, but the hydrophobic diameter of P4′ gradually increases with varying pH from 10 to 14, indicating its aggregation in solution and being sensitive to pH.

2.7. Effect of Ion Strength on Optical Properties. The influence of ion strength on spectra properties of conjugated electrolytes has been investigated to reveal properties of polymer in solution [23, 24]. Herein, we investigated the influence of ion strength on the optical properties of P4 and P4′. As shown in Figure 9(a), the emission spectra profiles of P4 remain unchanged with the addition of a series of concentrations of NaCl, particularly in the presence of 1 M NaCl. This exhibits the optical stability of P4 in the presence of high concentrations of salt, which may be mainly related to the formation of inner salt of P4 [25]. On the contrary, the addition of NaCl forces the change in the emission spectra profiles of P4′. The emission peak at 540 nm stemmed from BT unit gradually appears upon addition of NaCl. Adding NaCl into P4′ solution induces interchain aggregation due to electrostatic repulsion screening, which favors FRET from donor to acceptor and results in new emission band of BT units (Figure 9(b)). This conclusion reveals the optical stability of P4 upon addition of ions outperforms that of P4′.

2.8. Fluorescence Resonance Energy Transfer (FRET) Study. Since zwitterionic materials show excellent resistance against nonspecific biomolecules adsorption such as proteins and DNA [26], we studied FRET between P4/P4′ and

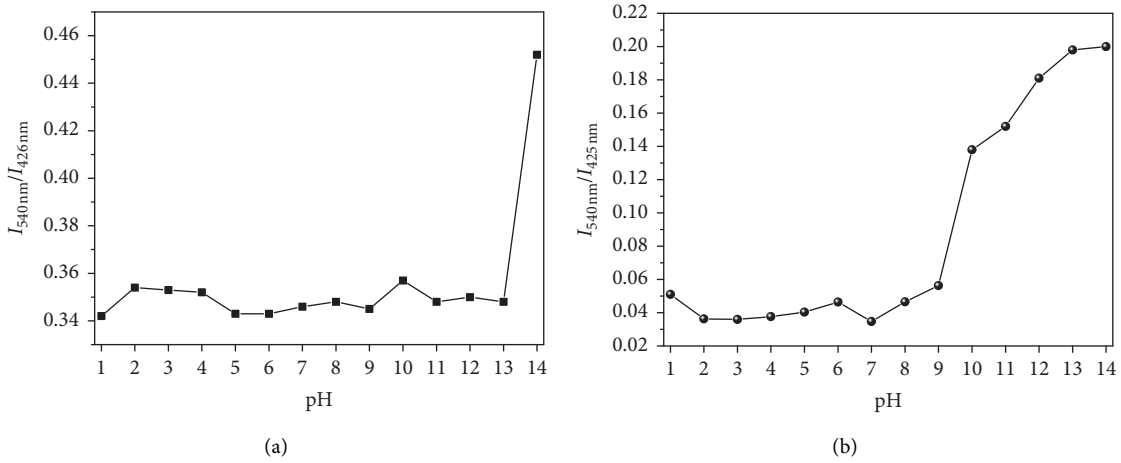

Figure 8: The value of $I_{540\ nm}/I_{426\ nm}$ for P4 (a) and P4′ (b) as a function of pH.

Table 1: DLS data of P4 and P4′ in water solution ([P4/P4′] = 10 μM).

pH		2	3	4	5	6	8	9	10	11	13	14
Hydrodynamic diameter/nm	P4′	29.98	28.54	36.39	36.39	36.39	37.87	36.39	43.92	50.65	53.22	115.8
	P4	32.27	33.56	36.39	35.78	30.84	32.03	36.39	28.00	27.2	43.66	50.67

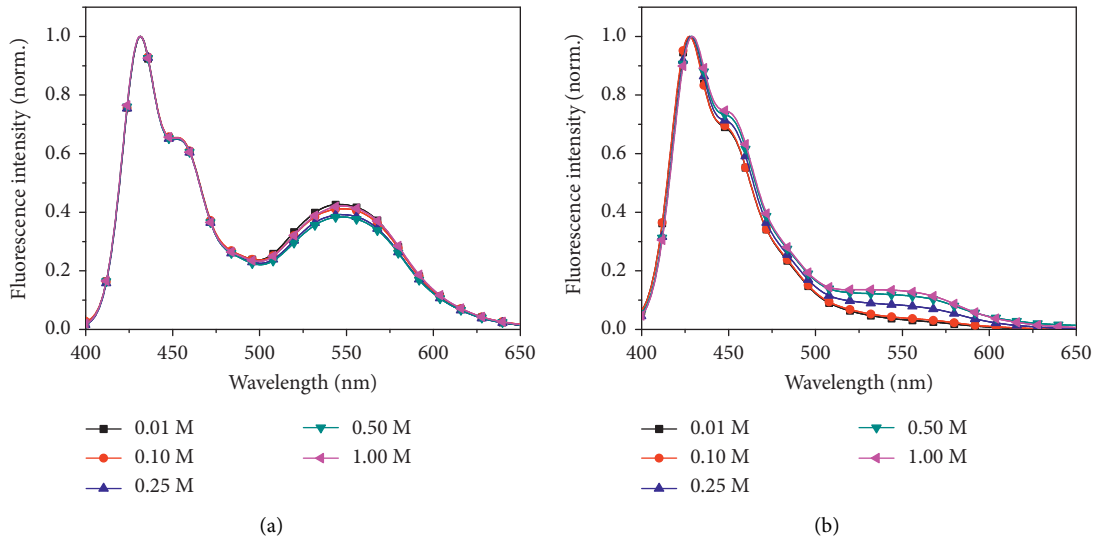

Figure 9: PL of P4 (a) and P4′ (b) in the presence of a series of concentrations of NaCl (excitation at 384 nm).

ssDNA-FAM. The mechanism of association of DNA molecules with cationic polymers is definitely electrostatic attraction, so we choose DNA as the candidate to investigate antifouling properties of zwitterion. PL experiments using ssDNA-FAM (5′-FAM-GCC TGG GAA AGT CCC CTC AAC T-3′) as the anionic energy-acceptor for P4 and P4′ were performed in 20 mM PBS (pH = 7.4) at [ssDNA-FAM] = 1.5×10^{-7} M (based on strands) and at [P4/P4′] = 1 μM. The samples were incubated for 5 min and the PL spectra were measured. Due to the efficient overlap between its absorption spectra and the emission spectra of polymers, FAM was selected as the label to favor FRET. FAM and FRET-induced dye emission are collected at 540 nm upon excitation of the polymer at 380 nm.

Increasing [P4] or [P4′], the PL spectra changes of ssDNA-FAM are given in Figures 10(a) and 10(b), respectively. Notably, FAM emission cannot nearly be observed for both systems. For P4′/ssDNA-FAM, it is clear that the FAM emission intensity gradually increases with the successive addition of P4′, whereas P4/ssDNA-FAM gives rise to no significant FAM emission, exhibiting the absence of FRET. Figure 11 vividly depicts optical properties of P4 in the presence of ssDNA-FAM in detail. The fluorescent discrepancies between two systems are generated from their

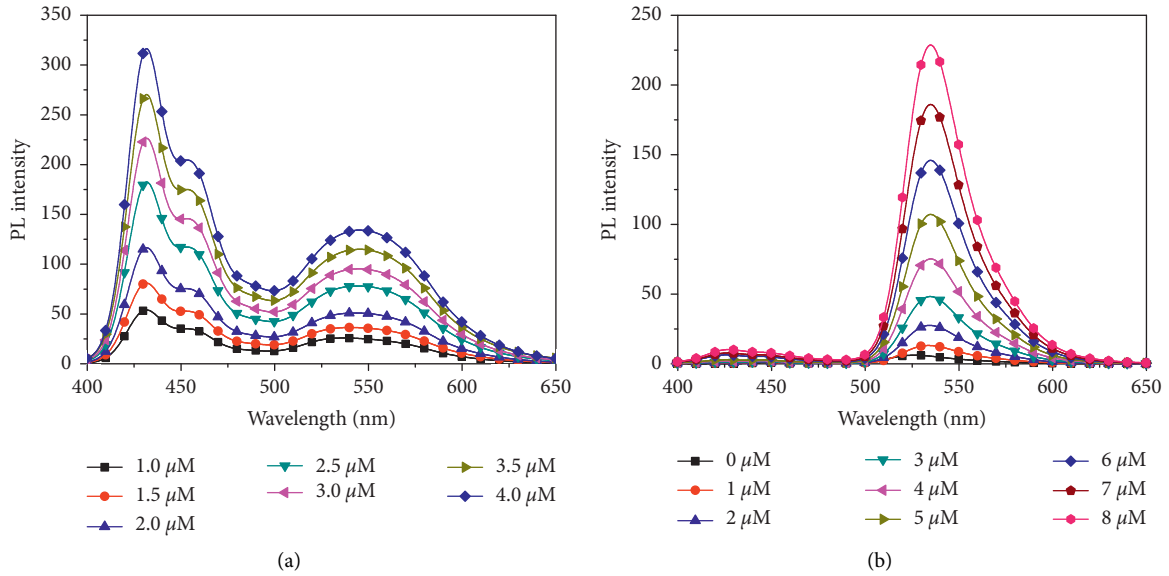

Figure 10: (a) The emission spectrum of P4/ssDNA-FAM solution upon increasing of [P4]. (b) The emission spectrum of P2/ssDNA-FAM solution upon increasing of [P4′] (excitation at 384 nm).

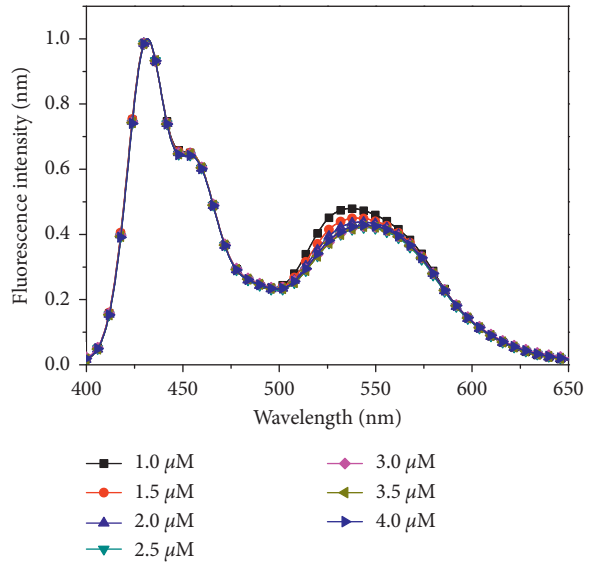

Figure 11: The normalized emission spectrum of P4/ssDNA-FAM solution upon increasing of [P4].

different effect to electrostatic interactions. For P4′, strong electrostatic forces between P4′ and ssDNA-FAM make complex more tight contacts, leading to efficient FRET. For P4, in addition to hydrogen bonding interactions, a more strongly bound hydration layer induced by electrostatically ionic solvation exists in the polymer solution, which endows the zwitterions with a high stability and a low fouling characteristic [27–29]. The absence of FRET between P4 and ssDNA-FAM highlights the resistance of zwitterions to biomolecules such as ssDNA-FAM. This result certifies that P4 may serve as antifouling materials with high specificity for biomedical applications relative to P4′.

To further verify that P4 has minimal nonspecific bindings with ssDNA-FAM, acceptor (ssDNA-FAM) quenching experiments were carried out under the same conditions as in the FRET experiments. The intrinsic emission properties of FAM were measured by direct excitation at 480 nm. When polymer concentrations are fixed at 2.0 μM, a 22% decrease in FAM emission intensity is observed for P4/ssDNA-FAM and a 76% decrease for P4′/ssDNA-FAM (Figure 12), indicating that zwitterionic polymer has minimal nonspecific adsorption inducing weakened interactions between P4 and ssDNA-FAM.

2.9. Cell Viability and Cell Uptake. To certify zwitterionic polymers (P4) have reduced cytotoxicity, we performed there in vitro cytotoxicity experiments using a standard

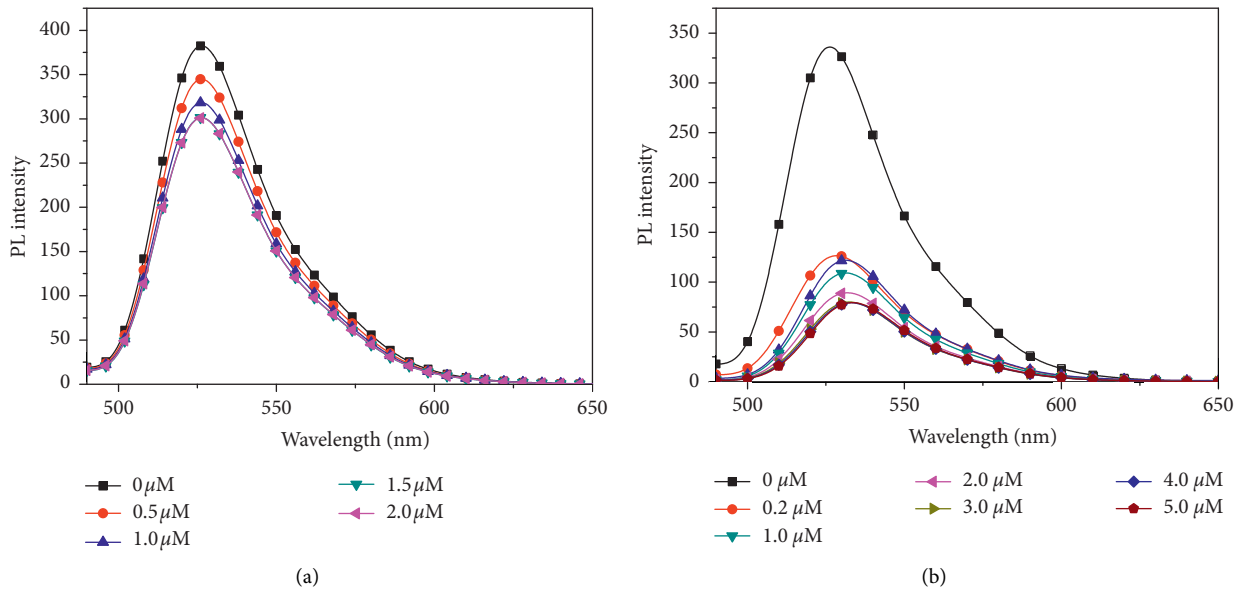

Figure 12: The emission of ssDNA-FAM in the presence of P4 (a) and P4′ (b) excitation at 480 nm.

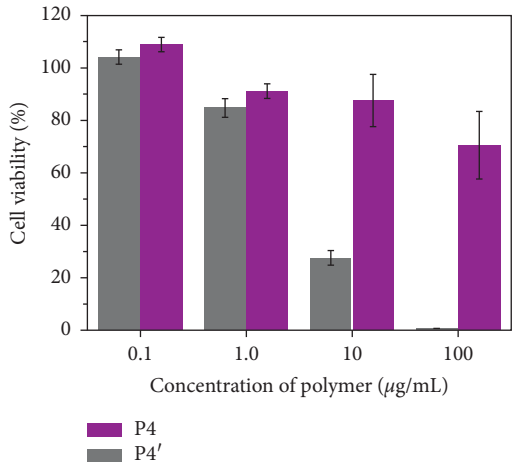

Figure 13: In vitro viability of ROW 246.7 cell exposed to P4 and P4′ solutions at concentrations of 0.10, 1, 10, and 100 μg/mL for 36 h.

3-(4,5-dimethylthiazol-2-yl)-2,5-diphenyltetrazolium bromide assay (MTT) on RAW 246.7 cell. These data clearly affirm the reduced cytotoxicity of P4 as compared to P4′ (Figure 13). Cell viability is able to be retained >80% even up to P4 concentrations of 0.01 mg/mL, showing higher biocompatibility and minimal cytotoxicity. Figure 14 exhibits the morphologies of cell exposed to a series of concentration from 0.1 to 100 μg/mL by fluorescence image. We clearly observe the aggregation of dead cell at P4′ concentration of 100 μg/mL as compared to P4. The higher cytotoxicity results from the fact that positive charge of P4′ side chains can disrupt lipid bilayers and finally kill cell [2, 30]. To ensure materials uptake by cells, low cytotoxicity is substantially valuable [31]. So we carried out cell uptake experiments of P4. A498 cells were exposed to a 0.1 mg/mL solution in DMEM medium (1 mL) solution for 2 h at 37°C with 5% CO_2. Then the cells were washed twice with PBS to remove polymers that do not penetrate into cell. The confocal laser scanning microscopy (CLSM) images of the sample are given in Figure 14, corresponding to the fluorescence image and fluorescence/transmission overlapped image, respectively. Visible blue fluorescence in the cells from Figure 14 (P4) shows that P4 can be taken up by cells, which should depend on an endosomal pathway [27]. On the contrary, P4′ is adsorbed on the surface of cells due to electrostatic interactions. The phenomenon should be ascribed to cell membrane disruption generated from the polycation migration and consequently the release of cell content as shown in Figure 14 [32–34]. Therefore, these results clearly demonstrate that zwitterionic polymers show cellular uptake ability and a very low cytotoxicity and may be promising for biomedical application such as drug delivery and long-term clinical application.

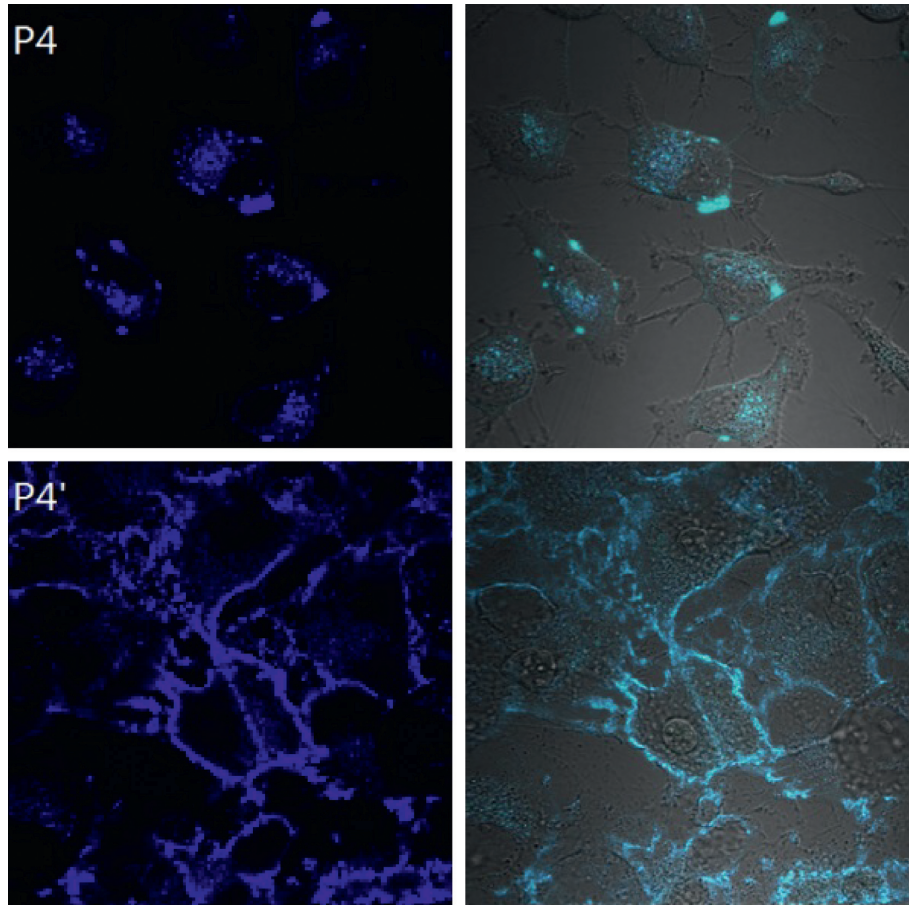

Figure 14: CLSM fluorescence and fluorescence/transmission overlapped images of A498 cells treated with 0.1 mg/mL polymer for 2 h. The signals are collected above 420 nm upon excitation at 380 nm for both P4 and P4′.

3. Conclusion

In this text, we design and synthesize two conjugated polyelectrolyte brushes with zwitterionic and cationic segments, respectively. Both polymers show better water-solubility, stronger optical stability and higher quantum efficiencies. As compared to cationic brush, zwitterionic brush is stable over the range of pH from 1 to 13 and in the high concentration of NaCl solution, showing stable optical properties of zwitterionic brush in complex media, which is an essential criterion for biological applications. FRET investigations greatly demonstrate that zwitterionic polymers have excellent resistance to biomolecules and thus antifouling characteristics. Most importantly, zwitterionic polymer is able to be taken up by RAW 246.7 cell and show their lower cytotoxicity, which is important for biological applications. Consequently, this work highlights an opportunity of exploiting conjugated polymer with ultralow fouling properties and low cytotoxicity to bring highly specific recognition or more efficient drug delivery system for biological applications.

Data Availability

The data used to support the findings of this study are included within the article and the supplementary information file.

Conflicts of Interest

The authors declare that they have no conflicts of interest.

Supplementary Materials

Supporting information for application of nanoscale zwitterionic polyelectrolytes brush with high stability and quantum yield in aqueous solution for cell imaging. Experimental general methods materials and synthesis of P1, P2, P3, P4, and P4′. (*Supplementary Materials*)

References

[1] M. L. Patil, M. Zhang, S. Betigeri, O. Taratula, H. He, and T. Minko, "Surface-modified and internally cationic polyamidoamine dendrimers for efficient siRNA delivery," *Bioconjugate Chemistry*, vol. 19, no. 7, pp. 1396–1403, 2008.

[2] A. Mecke, D.-K. Lee, A. Ramamoorthy, B. G. Orr, and M. M. Banaszak Holl, "Synthetic and natural polycationic polymer nanoparticles interact selectively with fluid-phase domains of DMPC lipid bilayers," *Langmuir*, vol. 21, no. 19, pp. 8588–8590, 2005.

[3] D. Li, A. S. Sharili, J. Connelly, and J. E. Gautrot, "Highly stable RNA capture by dense cationic polymer brushes for the design of cytocompatible, serum-stable SiRNA delivery vectors," *Biomacromolecules*, vol. 19, no. 2, pp. 606–615, 2018.

[4] J. Fang, B. H. Wallikewitz, F. Gao et al., "Conjugated zwitterionic polyelectrolyte as the charge injection layer for high-performance polymer light-emitting diodes," *Journal of the American Chemical Society*, vol. 133, no. 4, pp. 683–685, 2011.

[5] Q. Chen, Z. Li, B. Dong, Y. Zhou, and B. Song, "Zwitter-ionic polymer applied as electron transportation layer for improving the performance of polymer solar cells," *Polymers*, vol. 9, no. 11, p. 566, 2017.

[6] J.-J. Yuan, A. Schmid, S. P. Armes, and A. L. Lewis, "Facile synthesis of highly biocompatible poly(2-(methacryloyloxy) ethyl phosphorylcholine)-coated gold nanoparticles in aqueous solution," *Langmuir*, vol. 22, no. 26, pp. 11022–11027, 2006.

[7] Z. Cao and S. Jiang, "Super-hydrophilic zwitterionic poly(carboxybetaine) and amphiphilic non-ionic poly(-ethylene glycol) for stealth nanoparticles," *Nano Today*, vol. 7, no. 5, pp. 404–413, 2012.

[8] E. Muro, T. Pons, N. Lequeux et al., "Small and stable sulfobetaine zwitterionic quantum dots for functional live-cell imaging," *Journal of the American Chemical Society*, vol. 132, no. 13, pp. 4556-4557, 2010.

[9] L. L. Rouhana, J. A. Jaber, and J. B. Schlenoff, "Aggregation-resistant water-soluble gold nanoparticles," *Langmuir*, vol. 23, no. 26, pp. 12799–12801, 2007.

[10] J. Ding, H. Li, Y. Xie, Q. Peng, Q. Li, and Z. Li, "Reaction-based conjugated polymer fluorescent probe for mercury(ii): good sensing performance with "turn-on" signal output," *Polymer Chemistry*, vol. 8, no. 14, pp. 2221–2226, 2017.

[11] C. Wang, R. Zhan, K.-Y. Pu, and B. Liu, "Cationic polyelectrolyte amplified bead array for DNA detection with zeptomole sensitivity and single nucleotide polymorphism selectivity," *Advanced Functional Materials*, vol. 20, no. 16, pp. 2597–2604, 2010.

[12] H. Sun, J. Liu, S. Li et al., "Reactive amphiphilic conjugated polymers for inhibiting amyloid β assembly," *Angewandte Chemie*, vol. 131, no. 18, pp. 6049–6054, 2019.

[13] J. Wang, F. Lv, L. Liu, Y. Ma, and S. Wang, "Strategies to design conjugated polymer based materials for biological sensing and imaging," *Coordination Chemistry Reviews*, vol. 354, pp. 135–154, 2018.

[14] Z. Zhang, X. Lu, Q. Fan, W. Hu, and W. Huang, "Conjugated polyelectrolyte brushes with extremely high charge density for improved energy transfer and fluorescence quenching applications," *Polymer Chemistry*, vol. 2, no. 10, pp. 2369–2377, 2011.

[15] D. Yu, Y. Zhang, and B. Liu, "Interpolyelectrolyte complexes of anionic water-soluble conjugated polymers and proteins as platforms for multicolor protein sensing and quantification," *Macromolecules*, vol. 41, no. 11, pp. 4003–4011, 2008.

[16] K.-Y. Pu and B. Liu, "A multicolor cationic conjugated polymer for naked-eye detection and quantification of heparin," *Macromolecules*, vol. 41, no. 18, pp. 6636–6640, 2008.

[17] M. Wang, S. Zou, G. Guerin et al., "A water-soluble pH-responsive molecular brush of poly(N,N-dimethylaminoethyl methacrylate) grafted polythiophene," *Macromolecules*, vol. 41, no. 19, pp. 6993–7002, 2008.

[18] P. Mary, D. D. Bendejacq, M.-P. Labeau, and P. Dupuis, "Reconciling low- and high-salt solution behavior of sulfobetaine polyzwitterions," *The Journal of Physical Chemistry B*, vol. 111, no. 27, pp. 7767–7777, 2007.

[19] W.-C. Wu, W.-Y. Lee, and W.-C. Chen, "New fluorene-acceptor random copolymers: towards pure white light emission from a single polymer," *Macromolecular Chemistry and Physics*, vol. 207, no. 13, pp. 1131–1138, 2006.

[20] E. Vuorimaa, A. Urtti, H. Lemmetyinen, and M. Yliperttula, "Time-resolved fluorescence spectroscopy reveals functional differences of cationic polymer–DNA complexes," *Journal of the American Chemical Society*, vol. 130, no. 35, pp. 11695–11700, 2008.

[21] A. V. Dobrynin, R. H. Colby, and M. Rubinstein, "Polyampholytes," *Journal of Polymer Science Part B: Polymer Physics*, vol. 42, no. 19, pp. 3513–3538, 2004.

[22] R. Barbey, L. Lavanant, D. Paripovic et al., "Polymer brushes via surface-initiated controlled radical polymerization: synthesis, characterization, properties, and applications," *Chemical Reviews*, vol. 109, no. 11, pp. 5437–5527, 2009.

[23] Q.-L. Fan, Y. Zhou, X.-M. Lu, X.-Y. Hou, and W. Huang, "Water-soluble cationic poly(p-phenyleneethynylene)s (PPEs): effects of acidity and ionic strength on optical behavior," *Macromolecules*, vol. 38, no. 7, pp. 2927–2936, 2005.

[24] J. Wang, D. Wang, E. K. Miller, D. Moses, G. C. Bazan, and A. J. Heeger, "Photoluminescence of water-soluble conjugated polymers: origin of enhanced quenching by charge transfer," *Macromolecules*, vol. 33, no. 14, pp. 5153–5158, 2000.

[25] W.-F. Lee and Y.-M. Chen, "Poly(sulfobetaine)s and corresponding cationic polymers. VIII. Synthesis and aqueous solution properties of a cationic poly(methyl iodide quaternized styrene-n,n-dimethylaminopropyl maleamidic acid) copolymer," *Journal of Applied Polymer Science*, vol. 80, no. 10, pp. 1619–1626, 2001.

[26] Z. Zhang, J. A. Finlay, L. Wang et al., "Polysulfobetaine-grafted surfaces as environmentally benign ultralow fouling marine coatings," *Langmuir*, vol. 25, no. 23, pp. 13516–13521, 2009.

[27] J. Park, J. Nam, N. Won et al., "Compact and stable quantum dots with positive, negative, or zwitterionic surface: specific cell interactions and non-specific adsorptions by the surface charges," *Advanced Functional Materials*, vol. 21, no. 9, pp. 1558–1566, 2011.

[28] A. T. Nguyen, J. Baggerman, J. M. J. Paulusse, C. J. M. van Rijn, and H. Zuilhof, "Stable protein-repellent zwitterionic polymer brushes grafted from silicon nitride," *Langmuir*, vol. 27, no. 6, pp. 2587–2594, 2011.

[29] Y. Chang, Y.-J. Shih, C.-J. Lai, H.-H. Kung, and S. Jiang, "Blood-inert surfaces via ion-pair anchoring of zwitterionic copolymer brushes in human whole blood," *Advanced Functional Materials*, vol. 23, no. 9, pp. 1100–1110, 2013.

[30] A. Mecke, S. Uppuluri, T. M. Sassanella et al., "Direct observation of lipid bilayer disruption by poly(amidoamine) dendrimers," *Chemistry and Physics of Lipids*, vol. 132, no. 1, pp. 3–14, 2004.

[31] L. Vigderman, P. Manna, and E. R. Zubarev, "Quantitative replacement of cetyl trimethylammonium bromide by cationic thiol ligands on the surface of gold nanorods and their extremely large uptake by cancer cells," *Angewandte Chemie International Edition*, vol. 51, no. 3, pp. 636–641, 2011.

[32] J. T. Wilson, W. Cui, V. Kozlovskaya et al., "Cell surface engineering with polyelectrolyte multilayer thin films," *Journal of the American Chemical Society*, vol. 133, no. 18, pp. 7054–7064, 2011.

[33] Y. Wang, T. S. Corbitt, S. D. Jett et al., "Direct visualization of bactericidal action of cationic conjugated polyelectrolytes and oligomers," *Langmuir*, vol. 28, no. 1, pp. 65–70, 2011.

[34] Y. Wang, K. S. Schanze, E. Y. Chi, and D. G. Whitten, "When worlds collide: interactions at the interface between biological systems and synthetic cationic conjugated polyelectrolytes and oligomers," *Langmuir*, vol. 29, no. 34, pp. 10635–10647, 2013.